JOURNAL OF MECHANICAL ENGINEERING AND SCIENCES (JMES)
ISSN: 2289-4659 e-ISSN: 2231-8380
VOL. 15, ISSUE 2, 8029 – 8041
DOI: https://doi.org/10.15282/jmes.15.2.2021.08.0633

ORIGINAL ARTICLE

Variability analysis of ABS solid fuel manufactured by fused deposition modeling for hybrid rocket motors

J. A. Urrego P[1,*], F. A. Rojas M[1] and J. R. Muñoz L[2]

[1] Department of Mechanical Engineering, Universidad de los Andes Carrera 1 Este No. 19A-40 Ed. Mario Laserna, Of. ML 441 Bogotá Colombia
Phone: (57 1) 3394949
[2] Department of Physics, Universidad de los Andes, Cra. 1 No. 18A-10, Bloque IP 4976 Bogotá, Colombia

ABSTRACT – The process of fused deposition material (FDM) was used to manufacture propellant grains of Acrylonitrile Butadiene Styrene (ABS) as novel rocket fuel grain, with three types of geometry in the burning port. These solid fuel grains were used to measure the typical characteristics of combustion in rocket motors such as thrust and pressure inside the combustion chamber, seeking to obtain preliminary characteristics of operation and analyze the effect of combustion port geometry on pressure and thrust, using Multivariate Analysis of Variance (MANOVA) as statistical method. Two of the three geometries were manufactured with a helical-finocyl configuration, specially designed to be fabricated by Direct Digital Manufacturing (DDM), the other one was a straight-bore geometry also by DDM. This characterization experiment was performed on a static hybrid rocket engine, designed to inject 99.98% pure nitrous oxide into a combustion chamber with capacity to withstand 6.9 MPa of pressure, with an easy-to-exchange nozzle, avoiding erosive behavior in the throat. Statistical analyses made with the ABS fuel grains, suggest a significant effect on rocket motor pressure and thrust, due to helical geometric changes made to the combustion port of solid fuel grains made by FDM manufacture process.

ARTICLE HISTORY
Received: 16th Jan 2019
Revised: 24th Sept 2019
Accepted: 06th Dec 2019

KEYWORDS
Hybrid rocket motor; Multivariate analysis of variance; acrylonitrile; butadiene styrene; fused deposition modelling

INTRODUCTION

Recently, the aerospace industry has turned its attention back to the exploration and research of hybrid-type rocket propulsion systems. Using solid phase fuels and oxidants in liquid or gaseous phase has demonstrated high performance and versatility in combustion processes [1]. Some researchers have been interested in hybrid propulsion systems because of the attractive possibility of commercial uses and adaptability to long duration missions, re-ignition characteristics and good storability of non-toxic components with very low self-ignition capacity [2]. A significant number of hybrid rocket motors have been tested from 8 N to 1.11 MN thrust. However, larger hybrid production systems or larger hybrid production lines are not available, due to some disadvantages derived from the combustion process. It is now known that hybrid motors exhibit variable combustion behavior during operation, due to the manufacturing processes of the fuels used in them. Hybrids generally use HTPB (Hydroxyl-terminated polybutadiene) or Paraffin as fuel, which must be manufactured under processes of heating, casting or degasification. The nature of this process generates porosity and gas bubbles that can be controlled but not eliminated, which produces motor to motor variability during the combustion process [3].

On the other hand, the new processes of DDM (Direct Digital Manufacturing) have allowed the development of parts, pieces and prototypes with significantly complex geometries which can be produced quickly and with a wide variety of materials and dimensional tolerances of aerospace applicability [3, 4]. The implementation and utilization costs of these new polymer manufacturing technologies are decreasing due to the wide mass-market availability, making this manufacturing process very attractive for the development and research of propulsive systems [4]. The use of thermoplastic polymeric materials to manufacture fuel grains in hybrid propulsion systems, is a concept that has been recently studied and few studies of statistical variability in motor combustion performance have been reported. In addition, manipulation of some geometric features in fuel grains can improve the combustion performance in hybrid rocket motors, extending its applicability, reliability and general use in the aerospace industry [5–8].

This study seeks to use the advantages currently offered by DDM technology to develop polymeric fuels of wide availability and low cost. Specifically, this chosen technology facilitates the manufacture of complex geometries in solid fuel grain burning ports, which could not be easily achieved with traditional methods and materials of processing fuels for hybrid rocket motors. This experimental campaign used the FDM (Fused Deposition Modeling) methodology to generate solid fuel grains made of polymer ABS (Acrylonitrile Butadiene Styrene) to measure and analyze motor thrust and chamber pressure, which are obtained on a custom static test bench using nitrous oxide as oxidizer.

The current research focuses on analyzing the impact that variation of helical geometries in the burning ports of the ABS fuel grain exerts on the combustion performance of a hybrid rocket motor. To determine if there is an effect on the mentioned pressure and thrust variables caused by the different helical geometries, the statistical method called

*CORRESPONDING AUTHOR | J. A. Urrego P | ✉ jo-urreg@uniandes.edu.co

Multivariate Analysis of Variance (MANOVA) is used, which detects if there is a significant change in these variables due to geometry variations in the burning ports. The study of the performance variability and influence of geometry on the combustion port of ABS hybrid rocket engines, could be beneficial in optimizing processes for small/medium scale rocket propulsion systems (i.e. orbital control or satellite trajectory).

METHODS AND MATERIALS

Fuel Grain of Acrylonitrile Butadiene Styrene (ABS)

A wide variety of studies have been developed on hybrid rocket engines, especially with HTPB (Hydroxy-terminated Polybutadiene) as fuel, obtaining several results closely linked to the manipulation of characteristics such as mixture percentages (HTPB + curative agent), amount of gas retained during solidification and temperature. Under normal manufacturing conditions a grain of HTPB requires up to 15 days to cure completely. After curing, its solidified geometry cannot be modified and currently is not recyclable or reusable [5]. In addition, some countries have prohibitions on their importation, commercialization and legal manipulation, which impose restrictions on their use at least for research purposes.

As an alternative fuel grain, Acrylonitrile Butadiene Styrene (ABS) is proposed as a low-cost material with extensive production worldwide and is recyclable multiple times [6, 9]. The worldwide ABS production rate reported 10.8 million-ton since 2016, offering a good availability of this material for use in these propulsive systems [10].

Currently, ABS is not classified as a material used in rocket propulsion systems, however, Withmore et.al [11] reports an ABS combustion performance significantly close to HTPB in preliminary characterization experiments. His study obtained lower performances of only 4.6% for thrust and 7% for specific thrust compared to HTPB. In conducting properly laboratory experiments and acknowledging that the monomer ratio presently contained in commercial ABS would not give the optimum energy content, Withmore demonstrated in ABS a promising performance as a solid rocket fuel, with the benefits of its broad market accessibility and present versatility for processing and manufacturing [11].

In this case study, the FDM is used as an alternative that offers the possibility of manufacturing geometrically complex and structurally consistent ABS fuel grains [12]. This particular manufacturing process can easily produce geometries in the combustion ports; in contrast, these geometries are difficult or time consuming to produce by traditional casting methods. Additionally, the ABS can provide a significant advantage by improving regression rates in hybrid rocket engines, reduces the variability in the performance of hybrid motors because it offers greater structural homogeneity offering availability solutions in countries with restrictions on the use of controlled substances of this nature [5, 13].

Experimental Setup for ABS Fuel Grain Combustion Test

The objective of this research is to make an experimental comparison between fuel grains of ABS with three different combustion port geometries, obtained through an FDM manufacturing process. Several tests were performed on ABS grains of identical size on a static test bench developed by Universidad de Los Andes and tested at the Universidad de San Buenaventura in Bogotá. This section details the construction and assembly aspects of the test engine and the manufacturing processes of the test fuel grains.

Motor Case and Igniter Assembly

An experimental hybrid motor was built for testing of solid fuels grains. Figure 1 shows the cross section of the rocket-motor designed for the tests. To initiate the flame, an igniter based on 30 g of magnesium-potassium nitrate was placed directly into the pre-combustion chamber. Nicrom-based electronic matches (E-matches) start the igniters with a 12 V signal sent from the Data Acquisition and Control Console (DACC). E-matches and igniters are replaced after each test.

For pressure measurement during the test, a connection port was located on one side of the case, and a check valve was connected between the pressure transducer and the combustion chamber. An amount of 13 ml of Nuto H100-Mobil®oil was poured between the check valve and pressure transducer to reduce heat transfer during combustion, avoiding heat damage to the pressure sensor. Table 1 shows the main features of the hybrid rocket motor designed.

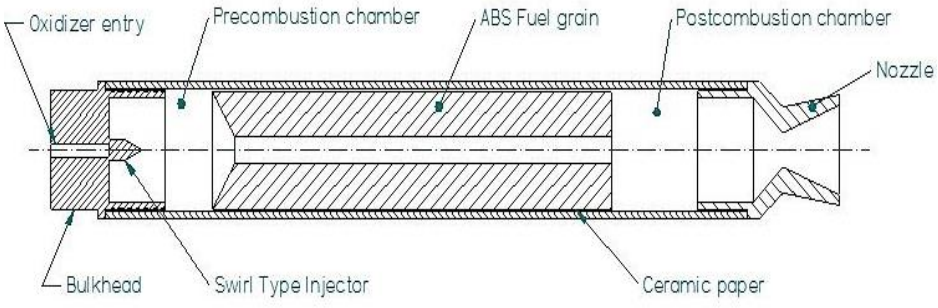

Figure 1. Cross section of the hybrid rocket case

Table 1. Main geometric hybrid rocket engine features [8]

Grain	Injector	Nozzle	Motor Case
248 mm Length	2.3 mm Diameter Orifice Nominal	21.5 mm Diameter Exit	365.02 mm Length
44.8 mm Diameter	2.3 mm Diameter Max. free passage	12.5 mm Diameter Throat	63.5 mm Diameter
12º conical inlet	BSJ Spiral Jet (Spraying Systems®)	2.95 Expansion ratio	3.5 mm Thickness

Instrumentation and Static Test Bench

An experimental static test bench for laboratory scale was built for this research. This device allows the direct measurement of pressure into the combustion chamber and axial thrust of the engine. This test stand supports a liquid nitrous oxide feed system that is regulated by a pressure regulator valve Victor SR 250D® at 3447 kPa outlet pressure and passes through a diaphragm GCE Druva MVR 500G® regulating valve flow control, to finally enter a D-Cryo-series® solenoid valve from Gems Sensors and Controls® excited with 12 VDC which is actuated from the DACC.

Figure 2 illustrates the test bench piping diagram. A Lexus loadcell® type S model SA (-200 N to 200 N) situated along the axial line measured the axial load of this motor. The output response of this sensor is 2.0 ± 0.2% mV/V and is excited with a 12 VDC source. The combustion chamber pressure was sensed with a Huba 520® (0 to 1 MPa) pressure transducer excited with 24 VDC and located next to the combustion chamber. The measuring systems were verified with controlled inputs and are reported in Table 2 with the installed calibration data for repeatability purposes [14].

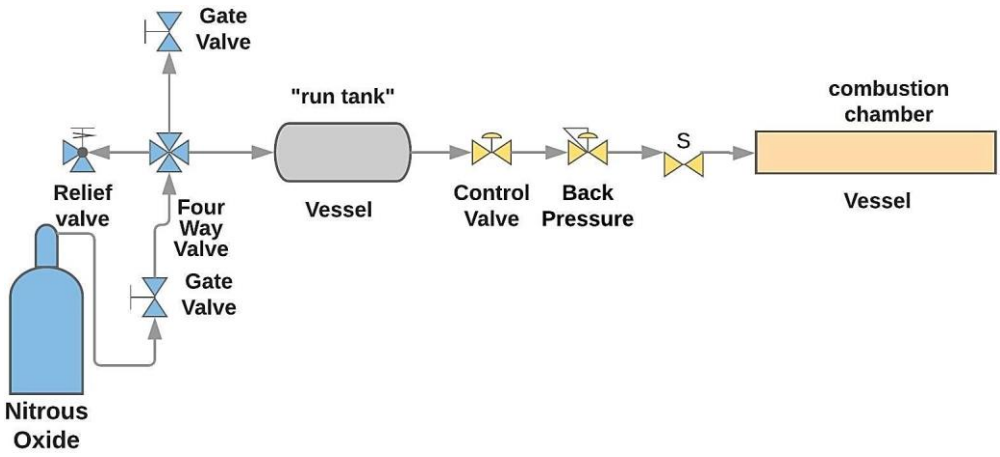

Figure 2. Experimental hybrid rocket piping scheme

Table 2. Manufacturer and installed accuracy for sensors used in the static test bench

Instrument Reference	Operating Range	Manufacturer accuracy	Installed test bench accuracy
Huba 520®	0-1 MPa	±0.25% FS	±1.2 kPa
Lexus® S type SA	(-200 N) - 200 N	±0.2% FS	±1.5 N

ABS Fuel Grain Manufacturing Process

The ABS fuel grains were manufactured with Prusa Tayrona FDM equipment, controlled by the Repetier Host software by Hot-World GmbH & Co. The extruded material was Shenzhen Esun Industrial Co.® commercial grade ABS filament, with an estimated monomer mole fraction of 50:47:3 (Butadiene: Acrylonitrile: Styrene). The manufacturing process produced a 100% solid ABS grain with an approximate mean weight of 270 g, a volumetric shrinkage of approximately 4.0%, 0.12% of mass gain by absorption of ambient humidity and no measurable deformation [11, 15].

The fuel grains were built with a 14.9 mm long conical inlet as a pre-combustion chamber to prevent erosive wear and chaotic combustion inside the combustion chamber [16]. Additionally, the grains were coated with alumino-silicate

ceramic fiber-based fabric (CeraTex®) to protect the motor case from the thermal damage. Relevant features of the printer configuration are shown in Table 3.

The selected geometries for the combustion port of solid grains were a straight-bore and finocyl configuration. However, the last one has two helical configurations, the first at 0.25 turns per inch (TPI) and the second at 0.125 TPI, which are difficult to obtain by traditional methods of casting, as shown in Figure 3. These configurations were selected to take advantage of the FDM manufacturing process, aiming to compare the combustion variability performance and the effect of manipulating the geometry of the port on the combustion performance of ABS solid grains obtained by DDM methods [17,18].

Table 3. FDM Equipment configuration for ABS fuel grain fabrication

Software	Infill	Equipment (General Features)
Slic3er Prusa Ed. 1.2.2 Repetier Host V2.0 RepRap Marlin/Sprinter (G-code flavor)	Fill density: 100% Fill pattern: Concentric Advance: Solid infill Threshold area: 70 mm^2	Filament diameter: 1.75 mm Filament density: 975 kg/m^3 Filament color: natural Temp. Extruder: 220ºC Temp. Hot-Bed: 95ºC Nozzle diameter: 0.4 mm

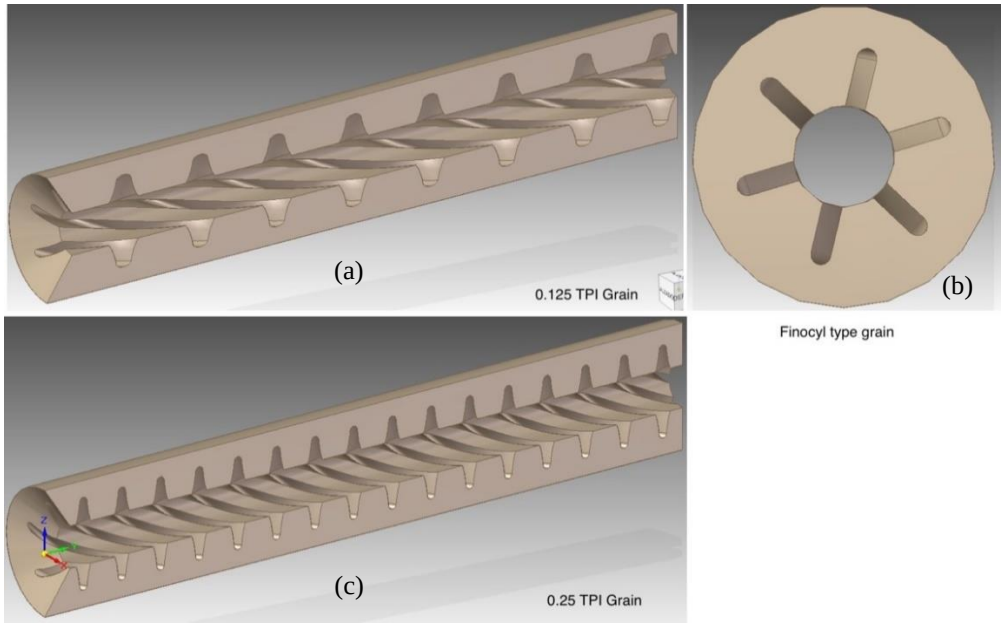

Figure 3. Helical configuration of finocyl ports for ABS fuel grains: (a) 0.125 TPI grain, (b) Front view of 0.125 TPI grain and (c) 0.25 TPI grain

THEORY

An Overview of Hybrid Rocket Combustion Performance

Inside the combustion in hybrid rocket engines, the gas-phase flow is restricted to the interior of the inner fuel grain surfaces, obtaining an internal tube flow. Parameters such as axial temperature, pressure, enthalpy, surface areas and mixing ratios may be factors affecting the boundary layer progression within the solid grain port [1], and the primary flow of gases from the combustion is accelerated axially along the combustion port and accumulated, producing pressure gradients inside the engine [11].

The most influential theory for understanding the burning process of hybrid engines was proposed by Marxman and Gilbert [16], that states the presence of a flame sheet inside the combustion port that generates heat transfer mechanisms which are the control mechanism of the combustion process inside a hybrid rocket engine, and takes place where the concentrations of fuel and oxidant are adequate to develop the combustion; however, these concentrations may not be stoichiometric.

As the combustion products approaches the nozzle, the normal fuel surface velocity gradients and the boundary-layer temperature become less influential, and the convective heat transfer rate reduces [1, 16, 19]. However, it is known that

inner flows with helical features have the capability to improve the burning rate. This is due to the augmented skin friction coefficient and the introduction of a centrifugal flow, which lowers the boundary layer thickness on the grain wall, bringing the flame nearer to the surface of combustion port, thereby improving the effectiveness of flame diffusion [20–22].

According to helical performance, Mishra and Gupta [23] proposed a study on solid fuels with a wide variety of helical geometries in their burn ports at different flow conditions for both laminar and turbulent. With these experiments they found a friction factor that allows to explain the increase of the regression rate in solid fuels with helical geometry ports. Thus, Eqs. (1) and (2) show a more specific model of the burning rate in a hybrid solid grain, including the skin friction coefficient for a straight flow field (Schoenherr-Schlicting model [20]) and a helical flow field (Mishra-Gupta model [23]).

$$\dot{r}_{helix} = \left(\frac{G_{ox}}{2 \cdot Pr^{2/3} \rho_{fuel}}\right) \cdot \left(\frac{\Delta h_{surface}}{h_v}\right) \cdot \left(C_{f_{helix}}\right) \cdot \left(\frac{1.27}{\beta^{0.77}}\right) \quad (1)$$

$$C_{f_{helix}} = C_{f_{straight}} + 0.0075 \cdot \left(\frac{D}{2 \cdot R_c}\right)^{0.5} \quad (2)$$

where,
$\dot{r}_{helix}$: Regression rate for helical geometries.
G_{ox} : Oxidizer mass flow.
Pr : Prandtl number.
$\Delta h_{surface}$: Convective heat transfer from the combustion flame.
h_v : Specific enthalpy of vaporization of fuel material.
β : Wall blowing coefficient.
$C_{f_{straight}}$: Local skin friction coefficient straight − bore
D : Instantaneous port diameter.
R_c : Helix radius of curvature.

Recently, the Kumar and Ramakrishna model suggested finding the fuel burning rate using the instantaneous combustion chamber pressure [24], which could be a promising and simple method to determine this performance parameter of a hybrid rocket motor. For now, it has been applied for straight-bore flow fields in HTPB fuel grains obtained by a casting method, but in future studies, this methodology could be adapted for the calculation of regression rates in helical geometries and ABS fuel grains.

RESULTS AND DISCUSSION

The ABS fuel grains with different geometry combustion ports were burned on the test bench, with a supply of nitrous oxide at approximately constant pressure and flow, obtaining the thrust-time and pressure-time graphs for 0.125 TPI, 0.25 TPI and straight -bore combustion ports as shown in Figure 4. The graphs a) to f) show the pressure and thrust peaks during the transient period of the engine start (0 to 1.8 s approx.), followed by the steady state behavior of the combustion process inside the thrust chamber. Additionally, Figure 4 g) presents the sectional cuts of the burned grains with the geometries respectively designed. The effect of the port geometry of ABS grains (statistically called treatment) on chamber pressure and thrust is studied using a random complete block experimental design (RCBD) to control for the effect of motor setup and maintenance routine after running six tests. The treatments used were: 1) helical geometry of 0.25 TPI, 2) helical geometry of 0.125 TPI and 3) straight-bore geometry. Twelve ABS fuel grains manufactured with FDM methods were burned, two with each geometry in two blocks which were tested in random order. The data of the test design is shown in Table 4.

Originally, the experiment was intended to have three blocks with two observations per treatment in each block. However, an issue occurred with the nitrous oxide supply line while running the second block, which generated statistical interactions between the second block and treatments; consequently, it was necessary to remove the block from the study and the model used to analyze data was fitted only with the first and third block.

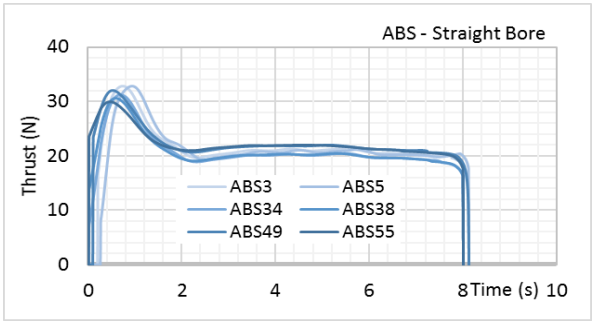

(a) Thrust-time of straight bore grain

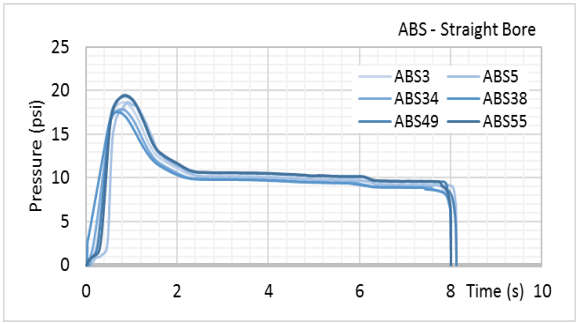

(b) Pressure-time of straight bore grain

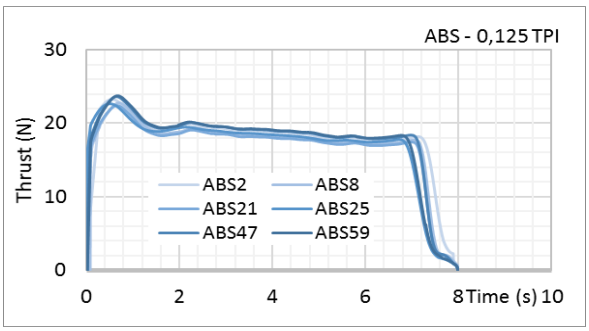

(c) Thrust-time 0.125 TPI grain

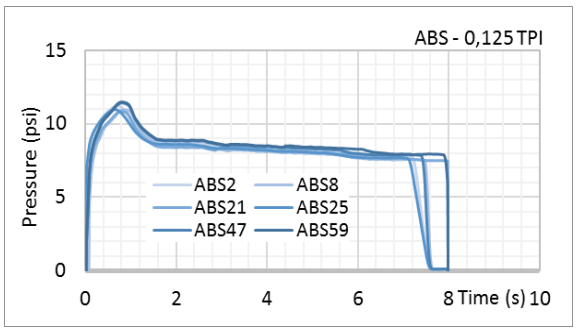

(d) Pressure-time 0.125 TPI grain

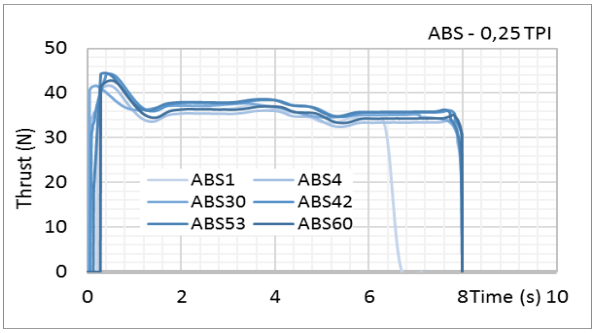

(e) Thrust-time 0.25 TPI grain

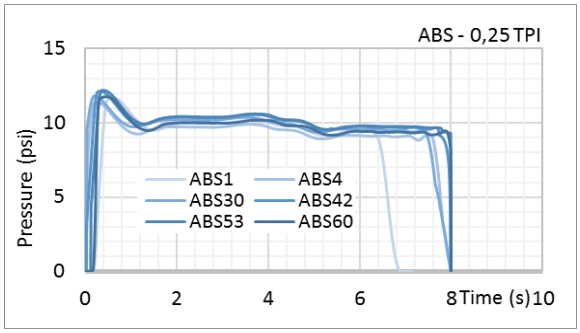

(f) Pressure-time 0.25 TPI grain

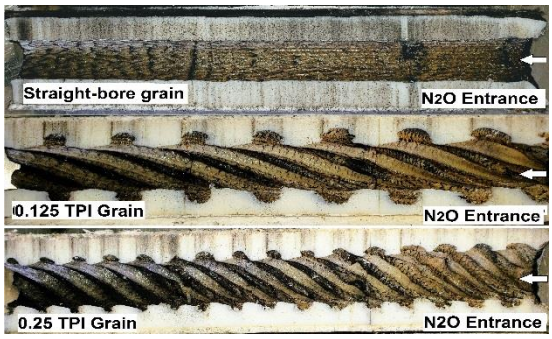

(g) Cross-section of fuel grains

Figure 4. (a) to (f) Thrust and pressure-time graphs and (g) cross-section of burned ABS fuel grains

Table 4. Characterization of experiment data

Obs. Number	Thrust N	Pressure PSI	Treatment (Geometry)	Block	Grain reference
1	20.910	10.018	Straight-Bore	1	ABS3
2	34.770	9.498	0.25 TPI	1	ABS4
3	20.666	9.916	Straight-Bore	1	ABS5

Table 4. Characterization of experiment data (cont.)

Obs. Number	Thrust N	Pressure PSI	Treatment (Geometry)	Block	Grain reference
4	35.716	9.794	0.25 TPI	1	ABS1
5	18.733	8.329	0.125 TPI	1	ABS2
6	18.218	8.096	0.125 TPI	1	ABS8
7	18.928	8.410	0.125 TPI	3	ABS47
8	21.614	10.377	Straight-Bore	3	ABS49
9	37.108	10.169	0.25 TPI	3	ABS53
10	21.679	10.424	Straight-Bore	3	ABS55
11	19.020	8.489	0.125 TPI	3	ABS59
12	35.655	9.776	0.25 TPI	3	ABS60

The distribution of response variables, thrust and chamber pressure, are analyzed with each treatment using adjusted box plots [25–27]. The Figure 5 (a) to (c) shows the box plots obtained for each variable (0.125 TPI,0.25 TPI and straight-Bore). In general terms, there is a skewness in both thrust and chamber pressure. Moreover, there are box plots with one whisker longer than the other, and the median, which is the horizontal line through the boxes, is shifted toward one of the box's edges indicating skewness in distributions.

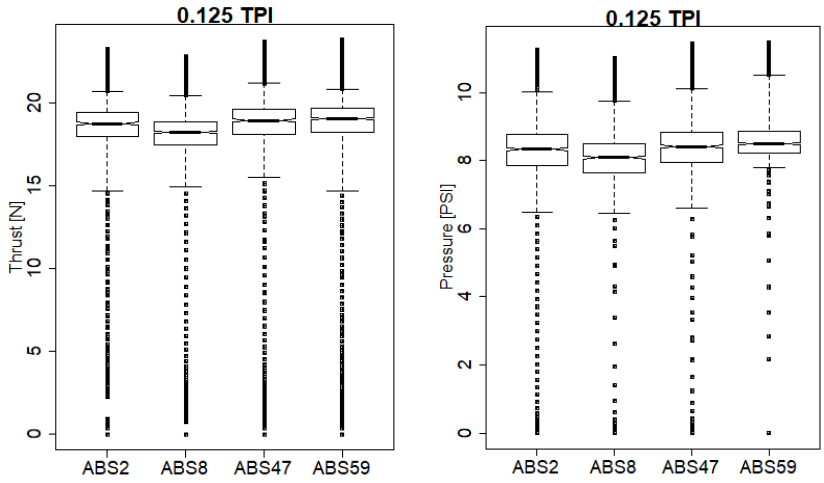

(a) Adjusted box plot for 0.125 TPI geometry

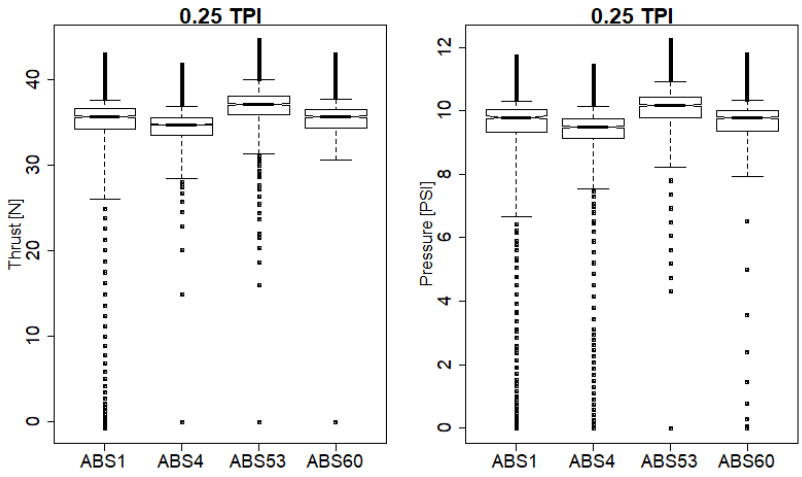

(b) Adjusted box plot for 0.25 TPI geometry

Figure 5. Adjusted box plots for each treatment

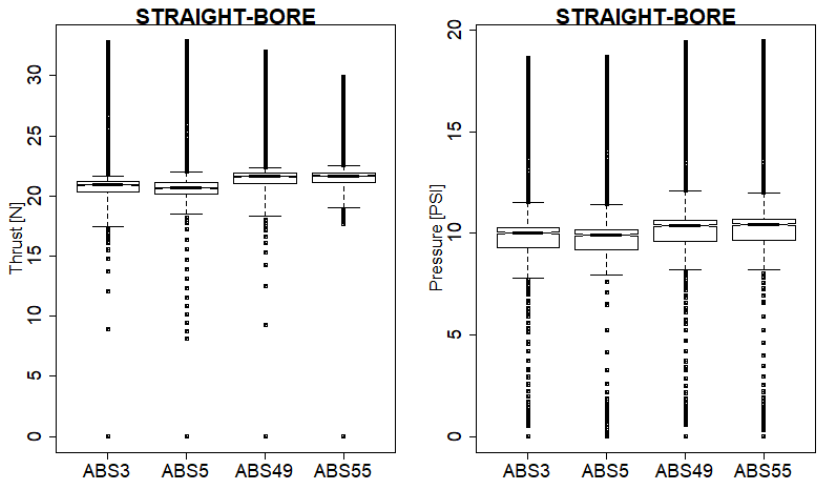

(c) Adjusted box plot for straight-bore geometry

Figure 5. Adjusted box plots for each treatment (cont.)

In addition to skewness, there are outliers in all distributions, indicated by points outside the whiskers' limits. Since all distributions have outliers and some are skewed, the median is used as a location estimator to analyze the results of the experiment (values presented in Table 5). To analyze if there is an effect of the combustion port geometry in the response variables vector (thrust and chamber pressure), the Multiple Analysis of Variance (MANOVA) model is used.

The MANOVA model states that [28]:

$$y_{ij} = \mu + \tau_i + \beta_j + \varepsilon_{ij} \tag{4}$$

where,

$$i = 1,2,\cdots a\ (Treatments)$$
$$j = 1,2,\cdots b\ (Blocks)$$

In Eq. (4) $\boldsymbol{y_{ij}}$ is the response vector (thrust, chamber pressure) with i_{th} treatment and j_{th} block, $\boldsymbol{\mu}$ is the general mean vector (thrust, chamber pressure), τ_i is the effect of i_{th} treatment (0.25 TPI, 1.125 TPI and straight-bore), β_j is the effect of j_{th} block and ε_{ij} is the multivariate normal random error term.

The hypothesis to contrast are:

$$H_0: \mu_1 = \mu_2 = \cdots = \mu_a \ vs\ H_1: at\ least\ one\ vector\ mean\ is\ different.$$

Additionally, MANOVA has assumptions that must be not violated. First it is important to check if there are multivariate outliers in the residuals of the model, since they may indicate possible problems. However, based on adjusted quantile [29], as shown in Figure 6, bottom right, outliers were not detected since all observations are showed in green. Observations in red are detected as outliers.

On the other hand, it is relevant to check if there is multicollinearity in the response variable matrix; MANOVA assumes that response variables are only moderately correlated. Since the condition index for response variable matrix is 7.56, which is less than 30, multicollinearity is not an issue [30–33]. To check normality assumption of residuals, thrust and chamber pressure residuals were checked with the Shapiro-Wilks test if normally distributed. The normal and P-values are 0.674 and 0.772 respectively, so there is not enough evidence to reject the null hypothesis of normality. Additionally, a Chi-Square with two degrees of freedom QQ plot is used to check if multivariate residuals are multivariate normally distribute. This can be done because Mahalanobis' square distance between each residual vector and the residuals mean vector **0** is Chi-Square distributed with two degrees of freedom if the multivariate residuals are normally distributed. The QQ-plot shows that there is no evidence of severe departure from normality since all points are between the dashed lines as shown in Figure 7.

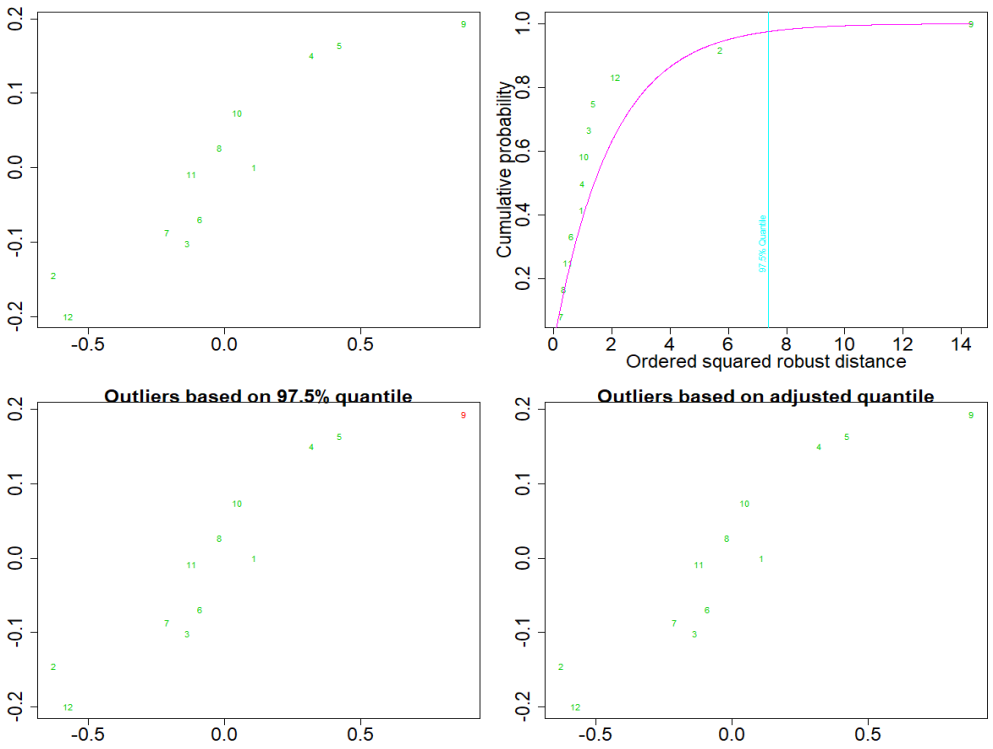

Figure 6. Multivariate outliers analysis

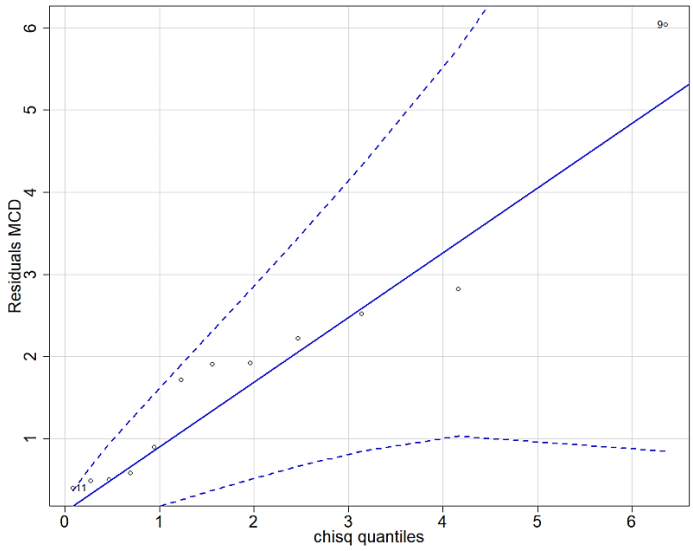

Figure 7. QQ Plot to evidence multivariate normal distribution

Additionally, to test the residuals homogeneity of variance assumption, the Box´s M test is used [34]. The test of homogeneity of residuals between treatments and between blocks is not significant because the P-values obtained are 0.2303 and 0.8601 respectively, indicating that there is not enough evidence to reject the null hypothesis of homogeneity. It is also important to check the linearity assumption between response variables per treatment; therefore, Figure 8 shows a scatter plot of the linear relationship between response variables showing the linear tendency in different color for each treatment. To generalize, residual analysis and multicollinear analysis of response variables do not present any significant problems. However, influential points are detected in observations 2, 9 and 12. Although these points have a significant impact, it was decided to continue the analysis of the model.

After checking the validity assumptions of the MANOVA model, its results are presented in Table 5. The MANOVA results with different methods show very small P-values, so there is enough evidence to reject the null hypothesis. This means that geometry of combustion ports in ABS fuel grains (treatments) has an effect on the response variables vector (thrust and chamber pressure), based on the experimental data.

On the other hand, based on the effect of response variables vector caused by the combustion port geometry, an exploratory study to analyze how thrust and chamber pressure are affected by the grain geometry is made by means of adjusted box plots [35].

As shown in Figure 9, the left panel box plots show that the medians are significantly different since the notches do not overlap, showing strong evidence of differences in the medians of thrust at a roughly 5% significance. 0.25 TPI geometry produces the highest median in thrust followed by straight-bore and 0.125 TPI grains [36].

Table 5. MANOVA results

Test	DF	Test Stat.	Approx. F	Num. Df	Den. Df	Pr (>F)
Pillai	2	1.9766	337.555	4	16	3.1513e-15 ***
Wilks	2	0.0000	1073.866	4	14	<2.22e-16 ***
Hotelling- Lawley	2	2217.3201	3325.980	4	12	<2.22e-16 ***
Roy	2	2174.7712	8699.085	2	8	4.4622e-14 ***

Signif. Codes: 0 ’ *** ’ 0.001 ’ ** ’ 0.01 ’ * ’ 0.05 ’ . ’ 0.1 ’_____’
DF: Degrees of freedom; num Df: numerator degrees of freedom; den Df: denominator degrees of freedom; Pr(>F): P-values

On the other hand, there is strong evidence that median pressure of straight-bore and 0.25 TPI grain are different from those produced by 0.125 TPI grain. These results agree with MANOVA analysis because they show that geometry affects both thrust and pressure, since their medians are not equal for all geometries. However, nothing can be concluded about differences in median between 0.25 TPI and straight-bore since the notches do overlap.

Additionally, box plots in Figure 9, also show that the 0.25 TPI grain thrust has more variability compared to straight-bore and 0.125 TPI grain, not only because of the middle half variability, but also in the range compared to 0.125 TPI grain and straight-bore when looking at the boxes’ upper and lower edges, and the upper and lower limits of the whiskers, respectively. It is also noticeable that the treatment with the lowest variability in thrust is produced by 0.125 TPI geometry.

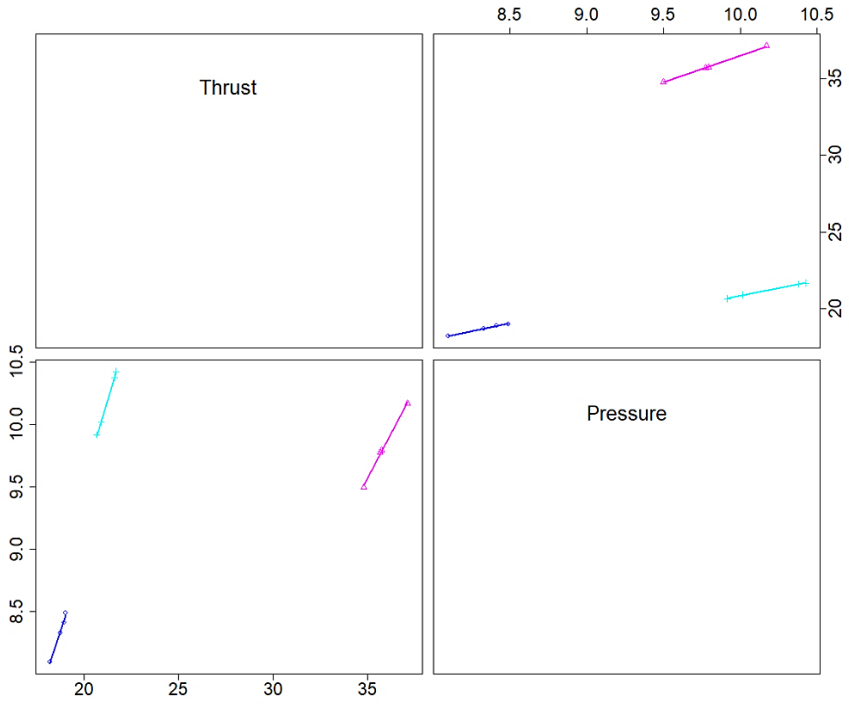

Figure 8. Scatter plot of linear relationship between response variables and treatment

Another relevant observation in the right panel in Figure 9, is that pressure has a lower middle half variability but a higher range with 0.25 TPI grain than straight-bore geometry. In contrast, 0.125 TPI geometry produces a lower middle half variability and range as well and has a left-skewed distribution. The 0.25 TPI grain and straight-bore produce more symmetric pressure distributions than 0.125 TPI. In general terms, pressure distributions have more spread than those for thrust distributions.

In general terms, the thrust produced by straight-bore geometry has a concentrated distribution, but it is lower than the distribution produced by 0.25 TPI and is barely surpassed by 0.125 TPI. It is also interesting that straight-bore produces

higher pressure similar to the 0.25 TPI but in contrast to the latter, the thrust produced is lower, probably due to interaction factors between the highly turbulent flow gas outlet conditions and the rocket engine thrust chamber design [37].

Finally, the thrust generated by the 0.25 TPI geometry has a higher range and middle half variability than other geometries. This agrees with a hypothesis around this behavior, which could be the generation of turbulent flow conditions and swirl components of greater magnitude within this geometry [22], compared with other treatments. However, this grain also exhibits greater variability, suggesting greater reactivity during the combustion process and higher heat transfer rates during burning [15, 20, 23, 25, 35]. Helical geometries directly affect the $\Delta h_{surface}$ and $C_{f_{helix}}$ terms of Eqs. (1) and (2), since the presence of highly turbulent flows induced by the internal geometry of grain, increase the diffusion efficiency of flame, the convective heat transfer rate in the fuel's multiphase (liquid-gas) combustion zone, and increasing the local skin friction given by the change in geometry and fuel texture obtained by default in the FDM manufacturing process [20–23].This behavior could be studied in the future, since it would allow for controlling the regression rate solely through geometric manipulation and local texture of the grain combustion port. Using this approach, it is possible to take advantage of the DDM methods, since the changes of geometry in the fuel grains and manipulation of combustion parameters may be done at low cost and in a technologically competitive way.

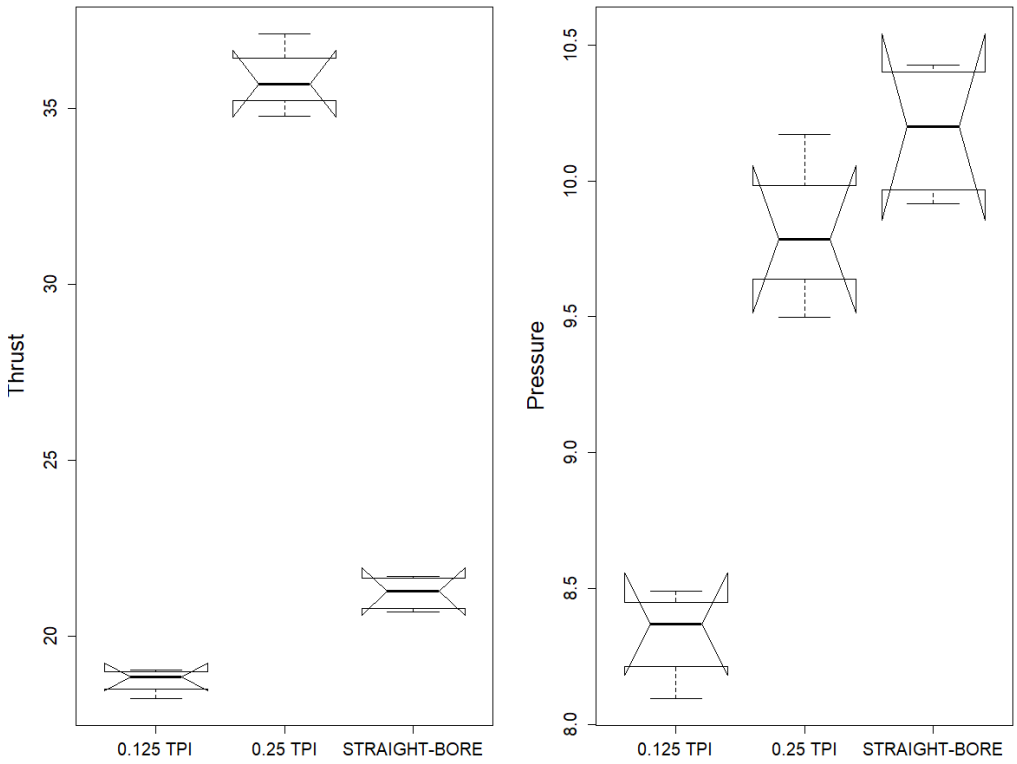

Figure 9. Box plots for thrust (N) and pressure (PSI) for different treatments

CONCLUSIONS

This experimental campaign demonstrated the possibility of using ABS and DDM methods for solid fuel grains production for small/medium scale hybrid rockets, whose burning ports were designed with helical geometries during the manufacturing process. The effect of the helical geometries of the burn ports on variables such as thrust and chamber pressure of the hybrid motor, was statistically evidenced under the MANOVA method.

These experimental tests showed higher thrust values for grains with 0.25 TPI geometry compared to grains with straight-bore and 0.125 TPI treatments. However, a greater variability of pressure and thrust in the 0.25 TPI treatment was also observed, suggesting a highly turbulent and high reactivity flow during the combustion process, due to rotational (swirl-whirl) flow components that could be involved during the burning of this grain, increasing its convective and radiative heat transfer rate, and also increasing the mass transfer rate producing a more reactive combustion. Although the 0.25 TPI treatment is the geometry that generates the greatest variability, its thrust and pressure are notably greater than the other treatments, which makes it an interesting geometry for further study in future research.

The actual performance in this experimental campaign, suggests an enhancement in ABS fuel burning rate with only geometric parameters variation. Clearly to confirm the relationship between flow kinetics and burn characteristics, it is necessary to perform a future specific regression rate measurement study, on these polymeric fuels with helical port geometries.

On the other hand, an interesting behavior was observed during the burning of straight-bore geometry, since it shows higher median pressure values than 0.125 TPI, but the thrust produced is just higher than produced by the 0.125 TPI geometry; this performance may be due to an interaction between the type of burning port geometry and the chaotic and turbulent flow of the exhaust gases through the nozzle throat. However, this ballistic characterization of the motor could be subject to computational fluid dynamics simulation and future experimental campaigns, aiming to optimize the rocket motor design for helical combustion ports in solid polymeric fuels. Similarly, a forthcoming study of the optimal polymer composition of ABS can be made to maximize fuel efficiency and increase its energy density as a rocket fuel.

In general terms, the fuel obtained with commercial ABS and DDM methods, currently offers a viable alternative for the development of small/medium scale hybrid rocket engines in countries with difficulty obtaining high performance rocket fuels.

ACKNOWLEDGEMENTS

This project is logistically supported by the School of Engineering of the Universidad de San Buenaventura-Bogotá. Thanks are extended to GasLab SAS and GasLab CEO Ing. Guillermo Ceballos for his advice and guidance during the experimental processes.

REFERENCES

[1] K. K. Kuo and M. J. Chiaverini, *Fundamentals of Hybrid Rocket Combustion and Propulsion*. American Institute of Aeronautics and Astronautics, 2007.

[2] G. Sutton and O. Biblarz, *Rocket Propulsion Elements*, 9th ed. Hoboken -New Jersey: John Wiley & Sons, 2017.

[3] J. McCulley, A. Bath, and S. Whitmore, "Design and testing of FDM manufactured Paraffin-ABS hybrid rocket motors," *48th AIAA/ASME/SAE/ASEE Jt. Propuls. Conf. & Exhib.*, no. August, pp. 1–24, 2012, doi: 10.2514/6.2012-3962.

[4] J. M. Waller, B. H. Parker, K. L. Hodges, E. R. Burke, and J. L. Walker, "Nondestructive evaluation of additive manufacturing state-of-the-discipline report," *Nasa/Tm-2014-218560*, no. November, pp. 1–36, 2014, doi: 10.13140/RG.2.1.1227.9844.

[5] S. A. Whitmore, Z. W. Peterson, and S. D. Eilers, "Comparing Hydroxyl terminated Polybutadiene and Acrylonitrile Butadiene Styrene as hybrid rocket fuels," *J. Propuls. Power*, vol. 29, no. 3, pp. 582–592, 2013, doi: 10.2514/1.B34382.

[6] J. V. Rutkowski and B. C. Levin, "Acrylonitirle-Butadine-Styrene complymers (ABS): Pyrolysis and combustion products and their toxicity-A review of the literature," *Fire Mater.*, vol. 10, no. July, pp. 93–105, 1986, doi: 10.1002/eat.20931.Psychometric.

[7] D. Rajamani and E. Balasubramanian, "Effects of heat energy on morphology and properties of selective inhibition sintered high density polyethylene," *J. Mech. Eng. Sci.*, vol. 13, no. 1 SE-Article, Mar. 2019, doi: 10.15282/jmes.13.1.2019.05.0375.

[8] A. Chafidz, M. Rizal, F. RM, M. Kaavessina, D. Hartanto, and S. M. AlZahrani, "Processing and properties of high density polyethylene/date palm fiber composites prepared by a laboratory mixing extruder," *J. Mech. Eng. Sci.*, vol. 12, no. 3 SE-Article, Sep. 2018, doi: 10.15282/jmes.12.3.2018.2.0333.

[9] P. Jindal, J. Jyoti, and N. Kumar, "Mechanical characterisation of ABS/MWCNT composites under static and dynamic loading conditions," *J. Mech. Eng. Sci.*, vol. 10, no. 3, pp. 2288–2299, 2016, doi: 10.15282/jmes.10.3.2016.7.0213.

[10] P. Insight, "ABS Plastic (ABS): Production, Market, Price and its Properties," 2018. [Online]. Available: https://www.plasticsinsight.com/resin-intelligence/resin-prices/abs-plastic/. [Accessed: 27-Jul-2018].

[11] S. A. Whitmore, Z. W. Peterson, and S. D. Eilers, "Analytical and experimental comparisons of HTPB and ABS as hybrid rocket fuels," *47th AIAA/ASME/SAE/ASEE Jt. Propuls. Conf. Exhib.*, no. August, pp. 1–48, 2011, doi: 10.2514/6.2011-5909.

[12] C. Bauer *et al.*, "Application of additive manufacturing in solid and hybrid grain design," 2016, doi: 10.2514/6.2016-4697.

[13] J. Rabinovitch, E. T. Jens, A. C. Karp, B. Nakazono, A. Conte, and D. A. Vaughan, "Characterization of PolyMethylMethAcrylate as a Fuel for Hybrid Rocket Motors," 2018, doi: 10.2514/6.2018-4530.

[14] J. A. Urrego P., F. A. Rojas M., and J. R. Muñoz L., "Combustion performance comparison of propellant grain for hybrid rocket motors manufactured by casting and fused deposition modeling," *Int. J. Mech. Eng. Robot. Res.*, vol. 8, no. 6, pp. 960–965, 2019, doi: 10.18178/ijmerr.8.6.960-965.

[15] S. A. Whitmore and S. L. Merkley, "Effects of radiation heating on additively printed hybrid fuel grain O/F shift," 2016, doi: 10.2514/6.2016-4867.

[16] G. Marxman and M. T. Gilbert, "Turbulent boundary layer combustion in the hybrid rocket," in *Symposium (International) on Combustion*, 1963, pp. 371–383, doi: 10.1016/s0082-0784(63)80046-6.

[17] J. A. Urrego Peña, "Research in experimental rocketry : study of influence of geometric and manufacture parameters in combustion of polymeric hybrid rocket fuel grains," Universidad de Los Andes, 2019.

[18] H. M. Lozada, A. Urrego, and F. Rojas, "Viability study of Acrylonitrile Butadiene Styrene Polymer as fuel for hybrid rocket engines in Colombia," *AIAA Propuls. Energy 2019 Forum*, no. August, pp. 1–17, 2019, doi: 10.2514/6.2019-3836.

[19] L. A. Arteaga M, "Design, construction and tests of a rocket propulsion motor with hybrid propellant in a static bank.," Universidad de Los Andes, 2018.

[20] S. A. Whitmore, S. D. Walker, D. P. Merkley, and M. Sobbi, "High regression rate hybrid rocket fuel grains with helical port structures," *J. Propuls. Power*, vol. 31, no. 6, pp. 1727–1738, 2015, doi: 10.2514/1.B35615.

[21] A. Bath, "Performance characterization of complex fuel port geometries for hybrid rocket fuel grains," p. 67, 2012.

[22] W. Treedet and R. Suntivarakorn, "Effect of various inlet geometries on swirling flow in can combustor," *J. Mech. Eng. Sci.*, vol. 12, no. 2, pp. 3712–3723, 2018, doi: 10.15282/jmes.12.2.2018.16.0328.

[23] P. Mishra and S. N. Gupta, "Momentum transfer in curved pipes," *Ind. Eng. Chem. Process Des. Dev.*, 1979.

[24] R. Kumar and P. A. Ramakrishna, "Measurement of regression rate in hybrid rocket using combustion chamber pressure," *Acta Astronaut.*, vol. 103, pp. 226–234, 2014, doi: 10.1016/j.actaastro.2014.06.044.

[25] M. Maechler *et al.*, "Package ' robustbase ' R topics," 2021.

[26] R Core Team, "R: A language and environment for statistical computing. R Foundation for Statistical Computing.," 2018. [Online]. Available: https://www.r-project.org.

[27] R. C. Team, "Microsoft R open." Microsoft, Viena-Austria, 2017.

[28] F. Qeadan, "On MANOVA using STATA, SAS & R. A short course in biostatistics for the Mountain West Clinical Translational," New Mexico, 2015.

[29] P. Filzmoser and M. Gschwandtner, "Mvoutlier. Multivariate outlier detection based on robust methods, R package version 2.0.9." 2018.

[30] M. Imdadulah and M. Aslam, "Mctest: An R Package for Detection of Collinearity among Regressors." 2016.

[31] M. U. Imdad and M. Aslam, "Mctest: Multicollinearity Diagnostic Measures," 2020.

[32] C. Montgomery, E. Peck A, and G. Vining, *Introduction to Linear Regression Analysis.*, 5th ed. New York: Jhon Wiley and Sons, 2012.

[33] D. C. Montgomery, *Diseño y análisis de experimentos*, 2nd ed. Limusa Wiley, 2006.

[34] A. R. da Silva, G. Malafaia, and I. P. P. Menezes, "Biotools: An R function to predict spatial gene diversity via an individual-based approach," *Genet. Mol. Res.*, vol. 16, no. 2, pp. 1–6, 2017, doi: 10.4238/gmr16029655.

[35] M. Hubert and E. Vandervieren, "An adjusted boxplot for skewed distributions," *Comput. Stat. Data Anal.*, 2008, doi: 10.1016/j.csda.2007.11.008.

[36] R. McGill, J. W. Tukey, and W. A. Larsen, "Variations of box plots," *Am. Stat.*, vol. 32, no. 1, pp. 12–16, May 1978, doi: 10.2307/2683468.

[37] M. Chiaverini and K. Kuo, *Fundamentals of hybrid rocket combustion and propulsion*, Second Edi. AIAA, 2008.